Biogeosciences Discuss., doi:10.5194/bg-2016-81, 2016
Manuscript under review for journal Biogeosciences
Published: 15 March 2016

Biogeosciences Discussions Open Access EGU

Tracer experiment and model evidence for macrofaunal shaping of microbial nitrogen functions along rocky shores

Catherine A. Pfister[1], Mark A. Altabet[2], Santhiska Pather[2], Greg Dwyer[1]

[1] Department of Ecology and Evolution, University of Chicago, Chicago IL, USA

[2] School for Marine Sciences and Technology, University of Massachusetts, Dartmouth, Bedford, MA, USA

Correspondence to: C. A. Pfister (cpfister@uchicago.edu)

Biogeosciences Discuss., doi:10.5194/bg-2016-81, 2016
Manuscript under review for journal Biogeosciences
Published: 15 March 2016

Abstract. The interdependence of macrofauna and microbes is increasingly recognized as a key feature affecting nutrient cycling. Tidepools are ideal natural mesocosms to test macrofauna and microbe interactions, and we quantified rates of microbial nitrogen processing using tracer enrichment of ammonium ($^{15}N_{NH4}$) or nitrate ($^{15}N_{NO3}$) when tidepools were isolated from the ocean during low intertidal periods. Experiments were conducted during both day and night as well as in control tidepools and those from which mussels had been removed allowing us to determine the role of both animal presence and daylight in microbial nitrogen processing. We paired time-series observations of ^{15}N enrichment in NH_4^+, NO_2^-, and NO_3^- with a differential equation model to quantify multiple, simultaneous nitrogen transformations. Mussel presence and daylight increased remineralization and photosynthetic nitrogen uptake. When we compared ammonium gain or loss that was attributed to microbes versus photosynthetic uptake, microbes accounted for 32% of this ammonium flux on average. Microbial transformations averaged 61% of total nitrate use; thus, microbial activity was almost 3 times photosynthetic nitrate uptake. Because it accounted for processes that diluted our tracer, our differential equation model assigned higher rates of nitrogen processing compared to prior source-product models. Our in situ experiments showed that animals alone elevate microbial nitrogen transformations two orders of magnitude, suggesting that coastal macrobiota are key players in complex microbial nitrogen transformations.

Keywords: tide pools, enrichment experiment, *Mytilus californianus*, differential equation model, nitrification, nutrient fluxes

Biogeosciences Discuss., doi:10.5194/bg-2016-81, 2016
Manuscript under review for journal Biogeosciences
Published: 15 March 2016

1. Introduction

Nitrogen cycle processes are carried out by a diversity of taxa, from microbes to macrofauna, that can all reside in the same habitat. Nevertheless, most studies tend to focus on characterizing and/or measuring the rate of only a single transformation at a time (e.g. nitrification or nitrate reduction), despite the co-occurrence of a diversity of nitrogen processes including those leading to loss or retention. Given an anthropogenic doubling over the past century of the supply rate of biologically available nitrogen to ecosystems (Galloway et al. 2008, Fowler et al. 2013) simultaneous with accelerated harvest of animals that recycle nitrogen (Worm et al. 2006, Maranger et al. 2008), it is essential that we understand the interacting contributions of microbes and macrobiota to nitrogen cycling. Using the experimental tractability of rocky shore tidepools as natural mesocosms, coupled with isotope tracer enrichments and mathematical modeling, we estimate here the rate of simultaneous nitrogen transformations as a function of animal abundance and time of day.

Along upwelling shores, the paradigm of productivity driven by upwelled nitrate has been challenged by studies quantifying the effects of animal excretion and regeneration (Dugdale and Goering 1967, Aquilino et al. 2009, Pather et al. 2014). It is well known that nitrogen regeneration is quantitatively significant in a variety of ecosystems (Schindler et al. 2001, Vanni 2002, Layman et al. 2010, Subalusky et al. 2014), However, to make a significant contribution to productivity, uptake of animal excreted ammonium by photo- and chemolithotrophs needs to be sufficiently rapid to retain nitrogen locally to avoid dispersion into the larger environment.

Biogeosciences Discuss., doi:10.5194/bg-2016-81, 2016
Manuscript under review for journal Biogeosciences
Published: 15 March 2016

69 Microbial nitrogen transformations are diverse, converting inorganic nitrogen among different
70 biologically available (NH_4^+, NO_2^-, or NO_3^-) or unavailable (N_2) forms. Accordingly, the
71 relative importance of these pathways also influences the retention or loss of regenerated
72 nitrogen. In coastal environments, there is increasing documentation that microbial nitrogen
73 transformation (e.g. chemolithotrophs) is intimately associated with nitrogen-regenerating
74 animals (Welsh and Castadelli 2004, Pfister et al. 2010, Heisterkamp et al. 2013, Stief 2013). We
75 know little about how these associations may impact nitrogen uptake by autotrophs. Rapid use of
76 animal-regenerated ammonium is likely by both obligate ammonia oxidizing microbes (e.g.
77 Ward 2008) as well as phototrophs that prefer it for energetic reasons (Magalhães et al. 2003,
78 Zehr and Kudela 2011). Accordingly, ammonium production by animals may be an important
79 contributor to the productivity along rocky shores of the northeast Pacific that are part of the
80 California Current Large Marine Ecosystem (CCLME).
81
82 There is parallel evidence that marine animals host diverse microbiomes (Pfister et al. 2010,
83 2014b, Miranda et al. 2013, Moulton et al. in press) as well as stimulate phototrophs with
84 excreted nitrogen (Taylor and Rees 1998, Plaganyi and Branch 2000, Bracken 2004). However,
85 we know little about the magnitude of animal impacts on nitrogen transformations. Incubating
86 seawater or sediment separate from the natural environment has provided controlled estimates of
87 single nitrogen transformations (e.g. Yool et al. 2007). However, a principle challenge has been
88 quantifying in situ the simultaneous nitrogen transformations that characterize natural
89 communities. Animal species may host nitrogen-metabolizing microbes while phototrophs in the
90 same environmental setting simultaneously compete for the animals' excreted ammonium. Light
91 levels controlling phototroph ammonium uptake may thus mediate nitrogen transformations.

Biogeosciences Discuss., doi:10.5194/bg-2016-81, 2016
Manuscript under review for journal Biogeosciences
Published: 15 March 2016

92

93 Here we quantify the influence of a common coastal marine animal, the California mussel, on the
94 overall magnitude of and the partitioning between simultaneous nitrogen transformations, using
95 tidepools at low tide as 'experimental mesocosms'. We use an experimental approach to test the
96 possible interacting roles of this animal and light on the rates of nitrogen transformations that, in
97 particular, influence net nitrogen retention. We manipulated the presence and absence of mussels
98 and light in combination with stable isotope tracer addition to directly test their effects on
99 nitrogen transformations. As with some other tracer experiments, (Tank et al. 2008, Peterson et
100 al. 1997), there were multiple fates for a single tracer addition, necessitating the use of
101 differential equations to simultaneously quantify multiple, simultaneous nitrogen processes. By
102 fitting model parameters with experimental data, we derive estimates for microbial nitrogen
103 transformations that are much higher than published rates where rate estimates are treated
104 singularly. We use the experiment and model to test whether nitrogen transformations in the
105 tidepools are elevated by mussels, inhibited by light, or affected by other environmental
106 variables. We also test for evidence of interactions between phototrophs and nitrogen-utilizing
107 microbes.

108

109 ## 2. Methods

110 ### 2.1 A Model for experimental data

111 Stable isotope enrichment experiments are an established methodology for quantifying nitrogen
112 processing in marine environments where the transfer of a tracer between source and product
113 pools is measured over time (Glibert et al. 1982, Lipschultz 2008). Typically, these assays are
114 done on seawater or sediments (e.g. review by Beman et al. 2011), though there are some

Biogeosciences Discuss., doi:10.5194/bg-2016-81, 2016
Manuscript under review for journal Biogeosciences
Published: 15 March 2016

115 examples where an organism is assayed (e.g. Heisterkamp et al. 2013). One acknowledged
116 challenge of these experiments is the simultaneous occurrence of multiple processes that can
117 dilute isotopically the source pool. For example, in a $^{15}NH_4$ tracer to estimate nitrification, the
118 ammonium tracer could be diluted by the production of unlabeled NH_4^+ by remineralization or
119 the microbial reduction of nitrite. Without accounting for isotope dilution, rates of transfer of
120 NH_4^+ to other pools would accordingly be underestimated. To assess the importance of isotope
121 dilution in our tidepool systems we compare rates of nitrogen transformation using two
122 approaches: (1) Using the previously used source-product model for a single transformation from
123 a ^{15}N-enriched source to a single product which does not account for isotope dilution (as
124 discussed in Glibert et al. 1982, Lipschultz 2008), and (2) Using a set of 6 differential equations
125 for modeling six different, simultaneous nitrogen processes which accounts for isotope dilution
126 in all relevant pools as well as the passage of tracer into intermediate pools.
127
128 The fates of 3 forms of inorganic nitrogen (ammonium, nitrite, nitrate) in an isolated tidepool
129 include a variety of processes mediated by microbes and other intertidal inhabitants, and are
130 illustrated in Fig 1. For ammonium, increases in concentration (and dilution of an enriched
131 tracer) can occur via excretion by animals and is represented by remineralization (m).
132 Phototrophs, both prokaryotic and eukaryotic, can assimilate ammonium and nitrate leading to
133 decreases in concentration, designated by uptake (u). Microbial transformations include
134 ammonium oxidation to nitrite (h), nitrite oxidation to nitrate (x), nitrate reduction to nitrite (y),
135 and nitrite reduction to ammonium (r). The parameter, m, is represented as a constant rate in our
136 model system whereas the other parameters are first-order rate constants in which the rate is the
137 product of the constant and the appropriate concentration. Because they are the first steps toward

Biogeosciences Discuss., doi:10.5194/bg-2016-81, 2016
Manuscript under review for journal Biogeosciences
Published: 15 March 2016

138 denitrification (production of N_2), both nitrite and nitrate reduction should be favored under low
139 oxygen conditions. Denitrification, in its entirety, nor anammox (which combines ammonium
140 and nitrite to produce N_2), are not explicitly modeled. Experiments to date that have utilized gas-
141 tight chambers have not detected nitrogen loss via N_2 gas production (unpublished data) and we
142 thus assume that nitrate and nitrite reduction were incomplete with respect to N_2 production and
143 consistent with nitrogen retention in the system.
144
145 The traditional source-product model generally involves estimating an average rate from time 0
146 to time t (Lipschultz 2008) and has the general form:
147 $$Rate = (R_k(t) - R_k(0))/[(R_s(0) - R_k(0)) * \Delta t] * [\bar{k}] \quad \text{Eq. (1)}$$
148 where *k* is the sink or product at time *t* (or the average $\bar{k}$), *s* is the source. Average product
149 concentration over the source of the experiment is $\bar{k}$ and *R* designates the atom % ($^{15}N/(^{15}N$
150 $+^{14}N)$ x100) of either the source or product component at the beginning of the experiment (0) or
151 the end (t). Equation (1) can be used to estimate individual nitrogen transformation rates
152 assuming little change in R_k. For example, ammonium oxidation to nitrite (*h* in Fig 1) is
153 estimated by adding $^{15}NH_4$ and monitoring the ^{15}N enrichment in nitrite. Nitrate reduction to
154 nitrite (*y*) is estimated by adding $^{15}NO_3$, and monitoring the ^{15}N enrichment in nitrite.
155
156 A recognized shortcoming of Eq. (1) is that multiple simultaneous processes (e.g. Fig. 1) can
157 change the concentration and isotopic composition of source and product nitrogen pools
158 (Lipschultz 2008). Resolving the influence of multiple, contemporaneous nitrogen
159 transformations requires a new approach that accounts for their influence over time on the
160 distribution of ^{15}N tracer. Pather et al. (2014) used an isotope dilution model (Glibert et al. 1982)

Biogeosciences Discuss., doi:10.5194/bg-2016-81, 2016
Manuscript under review for journal Biogeosciences
Published: 15 March 2016

that included simultaneous ammonium remineralization and uptake. Here, we extend that approach by constructing a differential equation model that includes all six simultaneous processes described above. We then fit our model to observed time-dependent changes in the concentrations and isotopic composition of ammonium, nitrite and nitrate. Because microbial metabolisms (*h, x, y, r*), phototroph uptake (*u*), and animal metabolism (*m*) should be occurring simultaneously, a major advantage of the differential equation model is that it estimates multiple, simultaneous processes.

In our differential equation model (Fig. 1), three differential equations describe how the concentrations of ammonium (A), nitrite (Ni), and nitrate (Na) in nmol L^{-1} change with time as a function of the 6 nitrogen flux terms.

$$\frac{dA}{dt} = m + r(Ni) - h(A) - 2u(A) \qquad \text{(Eq. 2)}$$

$$\frac{dNi}{dt} = h(A) + y(Na) - r(Ni) - x\,(Ni) \qquad \text{(Eq. 3)}$$

$$\frac{dNa}{dt} = x(Ni) - y(Na) - u(Na) \qquad \text{(Eq. 4)}$$

Ammonium remineralization (*m*) is assumed to be a constant rate independent of ammonium concentration. However, the other fluxes are first-order dependent on source concentrations with *h*, *u*, *r, x,* and *y* as the rate constants for ammonium oxidation, phototroph uptake, and nitrite reduction, nitrite oxidation, and nitrate reduction respectively. We also assumed that ammonium uptake (2*u*) was double that of nitrate uptake, a ratio reflecting the relative energetic ease of ammonium uptake by phototrophs (Thomas and Harrison 1985, Dortch 1990) and supported by measurements (Hurd et al. 2014). This 2:1 multiplier fit the data well across tidepool experiments and provided better fits than a higher or lower multiplier for ammonium:nitrate

Biogeosciences Discuss., doi:10.5194/bg-2016-81, 2016
Manuscript under review for journal Biogeosciences
Published: 15 March 2016

uptake. We note, however, that there are likely among species differences in *u* and its multiplier for ammonium uptake that need further study in marine macroalgae. By using only *u* to represent both phototrophic ammonium and nitrate uptake, we avoided an increase in the number of parameters and we simplified our model fitting routine. Although we initially set *u* to zero at night, we found that model fits were best when we let the model fit some phototrophic uptake at night, a phenomenon consistent with the observation that dark photosynthesis via carbon storage occurs in intertidal macroalgae (Kremer 1981). We excluded the uptake term (*u*) from nitrite dynamics because nitrite is at much lower relative abundance compared with ammonium and nitrate and is not known as a preferred nitrogen source for phototrophs. Finally, we note that *u* could also include uptake by heterotrophic bacteria. Based on the results presented below, however, phototrophic uptake appeared to dominate the *u* term. Given that nitrate and nitrite reduction are favored only at low O_2 concentration, it might be presumed that reducing processes are insignificant. However, tidepools with their natural complement of animals and algae, sediment, and small nooks and crannies likely have a high degree of spatial heterogeneity in oxygen and our results show significant rates of these processes.

Three equations model the time-varying concentrations (nmol $^{15}N\ L^{-1}$) of ^{15}N ammonium (n15A), nitrite (n15Ni), and nitrate (n15Na). $^{15}NH_4$ is diluted over time by remineralization (*m*) in the naturally occurring ratio of $^{15}NH_4$ to $^{14}NH_4$ of 0.00366. All other fluxes transfer ^{15}N from source to product in proportion to total nitrogen transfer:

$$\frac{dn15A}{dt} = m(0.00366) + r(n15Ni) - h(n15A) - 2u(n15A) \qquad \text{(Eq. 5)}$$

$$\frac{dn15Ni}{dt} = h(n15A) + y(n15Na) - r(n15Ni) - x(n15Ni) \qquad \text{(Eq. 6)}$$

Biogeosciences Discuss., doi:10.5194/bg-2016-81, 2016
Manuscript under review for journal Biogeosciences
Published: 15 March 2016

$$\frac{dn15Na}{dt} = x(n15Ni) - y(n15Na) - u(n15Na) \qquad \text{(Eq. 7)}$$

All parameter definitions are summarized in Table 1. Although isotope fractionation is known to occur for these nitrogen transformations, their magnitude is small compared to experimental enrichment values (e.g. Granger et al. 2008, Casciotti 2009, Granger et al. 2010, Swart et al 2014). We thus assumed that fractionation was insignificant in the context of this experimental manipulation and that first order reaction rate coefficients were equivalent for ^{14}N and ^{15}N containing forms of DIN.

We solved Eqs. 2-7 for the 6 parameters (*m, u, h, x, r, y*) simultaneously, by finding the best fits to the concentration and ^{15}N data for each experimental tidepool (see Sect 2.3). We further leveraged this experimental approach by comparing results for experiments carried out during the day and at night, and in tidepools with and without mussels, generating multiple parameter estimates and analyzing how they varied with environmental variables. To do so, we conducted all 4 experimental variants in each tidepool over the course of 2 months (daytime $^{15}NH_4$, nighttime $^{15}NH_4$, daytime $^{15}NO_3$, nighttime $^{15}NO_3$) (see Methods below).

2.2 Isotope enrichment experiments in tidepools

All isotope enrichment experiments were done in tidepools at Second Beach, a rocky north-facing bench 2 km east of Neah Bay, WA, USA (48°23' N, 124° 40' W) within the Makah Tribal Reservation. The experimental methods were described in Pather et al (2014), but are briefly reviewed here. Since 2002, California mussels (*Mytilus californianus*) have been removed from 5 tidepools while 5 others have remained as controls; in the year of this study, mussels were hand-removed (by cutting byssal threads) a month prior to the experiment to eliminate any

Biogeosciences Discuss., doi:10.5194/bg-2016-81, 2016
Manuscript under review for journal Biogeosciences
Published: 15 March 2016

biogeochemical signal of our presence. Besides this single perturbation, the pools have been left intact and contain a natural assemblage of macroalgae, microphytobenthos, surfgrasses *Phyllospadix scouleri* and *P. serrulatus* and macrofauna such as limpets, anemones, and fishes; the tidepools were 1.2 to 1.5 m above Mean Lower Low Water (MLLW) (Pfister 2007). The isolation of these tidepools for 5 to 6 hours during the low tide excursions both during daylight and nighttime hours during the summer of 2010 made it ideal to use the tidepools as intact mesocosms and probe the nitrogen transformations in natural ecosystems.

Four ^{15}N enrichment experiments within these 2 groups of tidepools provided a test of the fate of ammonium and nitrate, as a function of day and night hours (e.g. with and without photosynthesis), and the presence and absence of animals. The 'δ' notation is standard for expressing relatively low levels of ^{15}N enrichment as well as variations in natural abundance ^{15}N ($\delta^{15}N‰=[(R_{sample}-R_{atmN2})/R_{atmN2}] \times 1000$) and is used here for expressing measured values. For model calculations, $\delta^{15}N$ values were first converted to $^{15}N/^{14}N$ ratios and then to the concentration of ^{15}N by multiplying by the corresponding nutrient concentration. The four enrichment experiments included a target 1000‰ enrichment of either $\delta^{15}NH_4$ (added as 0.05M ammonium chloride, $^{15}NH_4Cl$) or $\delta^{15}NO_3$ (added as 0.05M sodium nitrate, $Na^{15}NO_3$), thus doubling either the $^{15}N\text{-}NH_4^+$ or $^{15}N\text{-}NO_3^-$ concentration during both a daytime low tide (25 Jun 2010, ~0715 to 1245 and 27 Jun 2010, ~0730 to 1300h), and a nighttime low tide (~2000 to 0145h on 13-14 Aug 2010 and 2150 to 0400h on 15-16 Aug 2010). A six-week interval between daytime and nighttime experiments was necessary due to the timing of low tides in the region. Strong nighttime low tide excursions only occurred in August, while daytime spring tides are ideal in June. These two experimental timepoints showed similar starting tidepool seawater

Biogeosciences Discuss., doi:10.5194/bg-2016-81, 2016
Manuscript under review for journal Biogeosciences
Published: 15 March 2016

temperatures (11.4 in Jun versus 11.3°C in Aug) and similar DIN concentrations (20.0 and 23.1 μmolL^{-1}). Both ammonium and nitrate concentrations in tidepools are typically high (>10 μmolL^{-1}) minimizing any concentration-related effects from tracer addition. Tidepool volume had been estimated previously with addition of a known amount of blue food coloring (e.g. Pfister 1995) and averaged 57.1 L with a range of 26.1 to 97.4 L. Deviations in our target of 1000‰ initial enrichment occurred due to natural variation in nutrient concentrations at the time of tracer addition, as well as error in tidepool volume estimates.

In all experiments, a water sample prior to tracer addition was collected to verify natural abundance isotope levels (T_o). After tracer solution was added and stirred, a sample of water was immediately taken to estimate actual initial enrichment (T_1). A second sample was taken ~ 2 h later (T_2), followed by a final sample after ~5 h (T_3), resulting in 3 samples to estimate the time course of concentration and ^{15}N enrichment in NH_4^+, NO_2^-, and NO_3^- in tidepool water. Although it would have been ideal to have greater than 4 samples to precisely describe the time course of ^{15}N through time, this number represented a cost-effective number across ten replicate tidepools and four experiments, and minimized investigator disturbance during the experiment. For each sample, we filtered ~180 ml of tidepool water through a syringe-filter (Whatman GF/F) into HDPE bottles, which we kept frozen until analysis. All nutrient concentrations were analyzed at the University of Washington Marine Chemistry lab, while isotope determinations were done at University of Massachusetts, Dartmouth. Methodology for nutrient and isotopic composition was reported previously (Pather et al. 2014, Pfister et al. 2014a). Nighttime sampling was done using headlamps, and took only 2-5 min, resulting in negligible illumination near tidepools. Tidepool

Biogeosciences Discuss., doi:10.5194/bg-2016-81, 2016
Manuscript under review for journal Biogeosciences
Published: 15 March 2016

oxygen, pH and temperature (Hach HQ4D) were also collected at ~ 2 h intervals throughout the experiment, and all tidepools had a HOBO temperature logger recording at 10 min intervals.

2.3 Fitting the Differential Equation Model to Data

Each tidepool experiment had 3 time points for nitrogen isotope composition and concentration, allowing parameter fits to be made to our model for each experiment. We solved our differential equations using the 'ode' function of R (in the deSolve R package, Version 3.1.0, www.r-project.org, Soetaert et al. 2012). The fit of our model to the data was calculated with the 'modCost' function of the FME package, which calculates the sum of the squared errors between the model and the data. We fit the model to the data using the 'modFit' function that uses a Levenberg-Marquardt minimization algorithm (Soetaert et al. 2010). As we did this estimation for each experiment, not treatment averages, we were able to examine stoichiometric relationships between nitrogen fluxes maintained at the scale of individual tidepools. Though the fitting routine always converged, we further tested the robustness of the fitting routine in several ways. First, we randomly varied the initial values for the parameters 100 times, drawing initial values from uniform distributions that allowed the parameter estimates to vary over several orders of magnitude (between 0 to 10). Because the *m* parameter was not first order and logically could be large, it ranged from 0 through 10^6. In all cases, the sum of squares of at least the best 10 parameter sets were within 10^{-3} (or less than 1-3% different), strongly suggesting that our fitting routine found the best parameter sets. As a second test of the model, we calculated net production or loss of ^{15}N by comparing the resulting total moles of ^{15}N from the observed values in each tidepool at the end of each experiment to the corresponding best-fit parameter estimates.

Biogeosciences Discuss., doi:10.5194/bg-2016-81, 2016
Manuscript under review for journal Biogeosciences
Published: 15 March 2016

290 Finally, we compared our differential equation model with the source-product model shown in
291 Eq. (1). Because our tracer experiments had 3 time points (T_1, T_2, T_3), we used the interval from
292 T_1 to T_2 to estimate the first paths for the transfer of tracer via oxidation or reduction (*h* and *y*)
293 and the interval from T_2 to T_3 to estimate the second oxidation or reduction process (*x* and *r*). In
294 this way, there was time for the tracer to become incorporated into nitrite before we estimated
295 the transformation rates of nitrite oxidation (*x*) in the case of enriched ammonium addition, or
296 reduction (*r*) in the case of enriched nitrate addition. Focusing our source-sink estimation on
297 these intervals allowed us to detect the greatest rate estimates from the source-sink model.
298
299 We measured multiple responses in our experimental manipulation. We analyzed all responses
300 with a linear mixed effects model using tidepool as a random effect and testing for a statistical
301 interaction between mussel presence and light (R, www.r-project.org).
302

303 ## 3. Results

304 ### 3.1 Isotope Patterns in experiments

305 After approximately 5 to 6 hours of isolation at low tide, results were dependent on both the
306 presence of mussels and the availability of sunlight (Fig. 2, Table 2). Ammonium concentration
307 was overall greater with mussels and during the day, and oxygen, temperature and pH all tended
308 to be greater during the day. Tidepool pH was lower at night ($p<0.05$) and possibly lower with
309 mussels ($0.10<p<0.05$). The dynamics of $\delta^{15}N_{NH4}$, $\delta^{15}N_{NO2}$, and $\delta^{15}N_{NO3}$ over the course of the
310 experiment revealed transfer of the tracer isotope and thus the action of microbial nitrogen
311 transformations. When $^{15}N\text{-}NH_4^+$ was added, enrichment in $\delta^{15}N_{NO2}$, and $\delta^{15}N_{NO3}$ was seen,

Biogeosciences Discuss., doi:10.5194/bg-2016-81, 2016
Manuscript under review for journal Biogeosciences
Published: 15 March 2016

312 though the presence of mussels diluted the $\delta^{15}N_{NH4}$ signal. Similarly, enrichment in $\delta^{15}N_{NH4}$ and
313 $\delta^{15}N_{NO2}$ followed the addition of $^{15}N\text{-}NO_3^-$ (Fig S1).
314
315 **3.2 The differential equation model estimates nitrogen transformation rates**
316 The advantage of using our tidepool experiments is that they contain the full range of actual
317 biological components and environmental fluctuations; but as they vary in the composition of
318 these components they also show individual differences. We thus fit the model to each tidepool
319 individually, rather than a mean value, allowing any influences due to environmental differences
320 to be incorporated into parameter estimates. ODE model predictions were generally highly
321 concordant with the observed nutrient and isotope data measured for each tidepool experiment
322 (Fig. 3). In addition to providing a good visual fit to the data for each tidepool (Fig. 3), the
323 estimated parameters predicted well the total amount of ^{15}N measured at the end of the
324 experiment (Fig. 4). Individual results deviated by as much as $\pm$20 nmol L^{-1}, but the estimated
325 and measured quantities were very similar and indicated the model showed no bias toward
326 producing or consuming ^{15}N (Fig. 3). The mean ^{15}N was 122.3 nmol total in the ammonium
327 enrichment experiments and 158.6 total in the nitrate enrichment experiments, indicating that
328 deviations were relatively modest (<16%), especially given the multiple sources of variability in
329 collecting and analyzing tidepool seawater.
330
331 **3.3 The significant effect of mussels and light on nitrogen processing**
332 The rates of ammonium remineralization in tidepools that we estimated with our ODE model
333 were greatest during the day when mussels were present, as was the uptake of ammonium (Fig.
334 2). In turn, all nitrogen metabolisms showed the greatest rates in the presence of mussels (Fig. 5,

Biogeosciences Discuss., doi:10.5194/bg-2016-81, 2016
Manuscript under review for journal Biogeosciences
Published: 15 March 2016

335 Table 3, Table 4). Further, all nitrogen transformations were greatest during the day with the
336 exception of nitrate reduction. For ammonium and nitrite oxidation (*h*A and *x*Ni), rates increased
337 an order of magnitude in the presence of mussels and during the day. As with all the microbial
338 transformations, nitrogen uptake attributed to all photosynthesizing species, from microalgae to
339 macroalgae and seagrasses, was greatest with mussels and also during the day. When we tallied
340 the percentage of ammonium flux due to microbes (nitrification + nitrite reduction) relative to all
341 the ammonium flux per tidepool (Table 3), we found that microbial ammonium flux accounted
342 for 32% of all ammonium flux when mussels were present and it was daylight. Similarly,
343 microbial nitrate flux was 61.4% of all nitrate flux. Although inorganic nitrogen concentrations
344 were always greater with mussels (Fig. 2), the rates of nitrogen transformations we estimated
345 were greatly affected by time of day and mussels (Figs. 2, 5, statistical summary in Table 4).
346
347 **3.4 Comparing the ODE model to single rate, source-sink models**
348 All rates of nitrogen transformation during the day and with mussels estimated with our
349 differential equation model (Eqs. 2-7) were greater than estimated by the traditional source-
350 product model (Fig. 5, Table 4). The ODE model always produced an estimate of the
351 ammonium oxidation rate far greater than that of the source-product model, particularly during
352 the day. The ammonium oxidation rate estimated with our differential equation model was
353 uncorrelated with the estimates from the source-product model (Spearman's r=0.004, Table 4).
354 Overall, there was little concordance between microbial nitrogen transformations estimated with
355 the ODE model and the source-product model, as the ODE model frequently estimated higher
356 rates (Fig. 5, Table 3).
357

Biogeosciences Discuss., doi:10.5194/bg-2016-81, 2016
Manuscript under review for journal Biogeosciences
Published: 15 March 2016

358 **3.5 Inferences about the relationships among nitrogen processes**

359 Parameter estimates from our model allowed us to assess the potential interaction among
360 nitrogen processes. We tested how model estimates of photosynthetic versus microbial
361 chemolithotrophic nitrogen use were related. If competition for ammonium occurs, then
362 ammonium oxidation (*h*) could be negatively related to phototrophic ammonium uptake (2*u*). To
363 avoid correlating parameters estimated simultaneously from the same model fitting attempt, we
364 correlated ammonium oxidation (*h*A) from the $^{15}NH_4$ enrichment with the uptake (*u*) from the
365 $^{15}NO_3$ experiments (and vice versa) and did not find a significant relationship in either case
366 (r=0.320, p=0.169 and r=0.297, p=0.200). The significant and positive relationship between
367 ammonium oxidation (*h*A) and remineralization (*m*) estimated from our differential equation
368 model (0.656, p<0.001) is likely not an artifact of unidentified parameters in the model. As
369 evidence, we note that ammonium oxidation in our ODE model was also positively related to
370 animal remineralization estimated independently, using the simple isotope dilution model from
371 Pather et al. (2014) (r=0.687, p<0.001). The positive relationship was unaffected by day or night,
372 indicating no enhancement of ammonium oxidation when photosynthetic ammonium uptake was
373 minimized.
374
375 Finally, we found few correlations between nitrogen transformation rates and oxygen,
376 temperature and pH in tidepools at the end of the low tide period. Only remineralization and
377 nitrogen uptake rates show a positive correlation with higher temperatures (r=0.423, p=0.009 &
378 r=0.432, p=0.008, respectively), primarily eukaryotic metabolic processes that increased with
379 temperature.
380

Biogeosciences Discuss., doi:10.5194/bg-2016-81, 2016
Manuscript under review for journal Biogeosciences
Published: 15 March 2016

381

382 ## 4. Discussion

383 ### 4.1 Animal and microbial contributions to nitrogen transformations

384 The remineralization of ammonium, oxidation and reduction of inorganic nitrogen, and the
385 uptake of ammonium and nitrate were all greater in tidepools with mussels versus those where
386 mussels were removed. Mean nitrate flux due to microbial processing (the sum of microbial
387 nitrate transformations in Table 3) ranged from 8 to 61% of the total nitrate uptake attributed to
388 both microbes and phototrophs, with the highest values when mussels were present and it was
389 daylight. Microbial processing accounted for an average 32% of the total ammonium flux with
390 mussels and daylight. Processing of both nitrate and ammonium by microbial chemolithotrophs
391 was thus significant in this rocky shore environment, and especially so when mussels were
392 present. Previous analysis of ammonium uptake in this system indicated that suspended particles
393 (e.g. phytoplankton) in tidepool seawater account for a negligible amount of ammonium uptake
394 (only 1-3 nmol L^{-1} h^{-1}) and microbial activity in tidepool seawater was an order of magnitude
395 less than benthic microbial activity (Pather et al. 2014). Additionally, benthic algae uptake rates
396 (estimated at ~5 x 10^{-4} h^{-1}, Pather et al. 2014) likely dominate the parameter *u*, though the
397 biomass specific uptake rates for the algae in our tidepools are unknown because we would have
398 had to destructively sample all algae to estimate this. However, published rates of ammonium
399 uptake in red algae ranged from 15900-62000 nmol per hour for every gram of algal dry weight,
400 while those for nitrate are 9700-28500 (Hurd et al. 2014). Thus, several individual algae could
401 account for the uptake of nitrogen that is not microbial, and our estimates of uptake using the *u*
402 parameter in the model are consistent with literature values (Table 3). In total, our enrichment
403 experiments indicate that microbial transformations can be as great as and even exceed the

Biogeosciences Discuss., doi:10.5194/bg-2016-81, 2016
Manuscript under review for journal Biogeosciences
Published: 15 March 2016

404 contributions of phototrophs to nitrogen dynamics. Further, the microbial activity related to
405 nitrogen cycling is primarily in association with benthic animals and phototrophs.
406
407 Previous genomic analyses showed that inert substrates (e.g. rocks) in tidepools with mussels
408 host a nearly identical microbial community to those in tidepools without mussels (Pfister et al.
409 2014b), while mussel shells themselves host a rich diversity of nitrogen-metabolizing microbial
410 taxa (Pfister et al. 2010). Combined with the nitrogen processing rates we quantified here, these
411 studies suggest that California mussels are loci for the microbial processing of nitrogen. Marine
412 invertebrates as hosts for significant nitrogen processing is further supported by work with snails
413 and other bivalves, which are demonstrated sites of nitrogen transformations including
414 ammonium oxidation (Welsh and Castadelli 2004, Stief et al. 2009, Heisterkamp et al. 2013).
415 N_2O production is also suggested for sediment-dwelling bivalves (Heisterkamp et al. 2013) and
416 those in sealed chambers (Stief et al. 2009). Evidence for bivalves as hotspots for nutrient
417 dynamics also includes species in river and stream environments (Atkinson & Vaughn 2014).
418 Mussels on rocky shores can average very high densities of 4661 individuals per m^2 (Suchanek
419 1979), suggesting that ammonium concentrations above mussels should be in mmol
420 concentrations (Pfister et al. 2010). Observation of much lower concentrations directly over
421 mussel beds (Aquilino et al. 2009), and in tidepools (this study) suggests the simultaneous
422 operation of other N processing pathways as observed here.
423
424 **4.2 Microbes contribute to nitrogen retention**
425 In high-energy coastal environments, animal regenerated ammonium could be advected by
426 waves and currents rather than retained. Because the rates we quantified are rapid, and because

Biogeosciences Discuss., doi:10.5194/bg-2016-81, 2016
Manuscript under review for journal Biogeosciences
Published: 15 March 2016

427 tidepool habitats are high flow refugia, net retention of inorganic nitrogen in nearshore areas can
428 result, a phenomenon that is likely to enhance local primary production. Over a diel cycle, both
429 ammonium and nitrite oxidation and nitrate and nitrite reduction occurred, and all are processes
430 that retain dissolved and biologically available nitrogen. Although we did not follow our tracer
431 into all tidepool species, previous analyses showed it was readily incorporated into tidepool algae
432 (Pather et al. 2014). Nitrogen loss processes were not quantified, though other experiments with
433 gas-tight chambers indicated no loss of nitrogen via enriched N_2 gas (Pfister & Altabet
434 unpublished data). Additionally, if the loss of ^{15}N signal was occurring due to anammox or
435 denitrification completed to nitrogen gas, then our models would have systematically estimated a
436 loss of ^{15}N, a result not supported by our analyses (Fig. 4). Further, phototrophic uptake of ^{15}N
437 was the only other term in the model for nitrogen loss. Our model predictions for uptake no only
438 were robust in both day and night experiments (Fig. 4), but the uptake rates were highly
439 consistent with measured uptake rates of marine algae (see section 4.1 above). We recognize,
440 however, that nitrogen loss processes via the production of the greenhouse gas nitrous oxide is
441 suggested in association with other animal species (Heisterkamp et al. 2013). Though the return
442 of nitrogen gas to the atmosphere is a significant feature of low oxygen, open ocean areas (Ward
443 2013) there was no evidence for it here. In this study, and in the analysis of naturally occurring
444 nitrogen isotopes (Pfister et al. 2014), nitrogen retention is instead suggested in high-energy
445 coastal areas, though the generality of this finding deserves further study.
446
447 Both nitrate and nitrite reduction rates were significant and are evidence for incomplete
448 denitrification or DNRA processes thought to be occurring only at low oxygen. Even during
449 daytime periods of high oxygen, nitrate and nitrite reduction were observed, suggesting that

Biogeosciences Discuss., doi:10.5194/bg-2016-81, 2016
Manuscript under review for journal Biogeosciences
Published: 15 March 2016

450 tidepools provide microsites where these microbial reducing processes can take place. The
451 oxidation of ammonium and nitrite, though not positively related to final oxygen level, was
452 greatest during the day and with mussels. Even at night when oxygen could be very low, there
453 was sufficient ambient oxygen to permit nitrification. Thus, even though remineralization
454 decreased at night and oxygen levels dropped, ammonium oxidation remained at an average of
455 160.6 nmol L^{-1} h^{-1} in the presence of mussels.
456
457 Although competition for ammonium between nitrifiers and phototrophs is poorly understood,
458 the preference for ammonium uptake may make it a contested resource. Sediment microalgae
459 have been shown to be competitively superior to ammonium oxidizing bacteria, likely due to
460 higher specific uptake rates and faster growth (Risgaard-Petersen et al. 2004). Here, we found
461 little evidence for competitive interactions for either ammonium or nitrate between
462 photosynthetic processes and microbial chemolithotrophs. Microbial transformations in the dark
463 did not increase, suggesting that microbial nitrogen metabolism is driven more by the stimulation
464 of animal excretion that occurs in these tidepools during the day, perhaps because of increased
465 tidepool temperature (Bayne & Scullard 1977). We also show no evidence of UV inhibition of
466 nitrification (e.g. Horrigan & Springer 1990, Guerrero & Jones 1995). We note also that
467 tidepool ammonium levels rarely were lower than several μM, and thus ammonium should not
468 have been depleted and limiting unless there are depleted microsites. Further studies at low
469 ammonium, including areas where animal regeneration is reduced and ammonium may be
470 contested, are warranted to understand how phototrophs and chemolithotrophs interact.
471
472

Biogeosciences Discuss., doi:10.5194/bg-2016-81, 2016
Manuscript under review for journal Biogeosciences
Published: 15 March 2016

473 **4.3 The Differential equation model captures rapid and simultaneous processes**

474 We developed the ODE model to simultaneously estimate multiple microbial transformation
475 rates and thus provide a more realistic descriptor of microbial activity in nature. Our model focus
476 on the rates of simultaneous nitrogen transformations assures that it is general and applicable to
477 any system. A key result here is that rate estimates from the differential equation model were
478 often much greater than those from the source-product model (Lipschultz 2008, and Glibert
479 1982). We suggest two reasons that our ODE estimated greater rates. First, the rapidity of
480 microbial transformations combined with the diversity of microsites in nature mean that tracer
481 enrichment can readily cycle through multiple products. Thus, ^{15}N in ammonium may be
482 oxidized not only to nitrite, but also to nitrate and then potentially reduced (Fig. 1). Our model
483 allows this 'cycling', whereas a source-sink model assumes a single source and product are
484 involved in the estimation of ^{15}N dynamics. The second reason our ODE model estimates greater
485 rates than a source-sink is that ammonium remineralization by macrobiota in nature can rapidly
486 dilute the $^{15}NH_4^+$ signal. A diluted $^{15}NH_4^+$ signal leads to underestimation of nitrogen dynamics
487 with source-sink models, a concern noted by its authors when source-product models were
488 derived. Here, and in Pather et al. (2014), we note that the effects of ammonium dilution were
489 most pronounced with mussels during the day, where all microbial rates were underestimated
490 with a source-product model. Our ODE model, in contrast, accounts for the propagation of tracer
491 dilution by ammonium remineralization to all DIN pools, likely resulting in greater estimates for
492 multiple nitrogen metabolisms. Indeed, our estimates of nitrification are several orders of
493 magnitude greater than those estimated in other coastal locales with source-product models
494 (Beman et al. 2011), allowing us to conclude that macrobiota greatly enhance rates of nitrogen
495 transformations. We further note that the rates we quantified are characterized by high variability

Biogeosciences Discuss., doi:10.5194/bg-2016-81, 2016
Manuscript under review for journal Biogeosciences
Published: 15 March 2016

among tidepools, a result likely due to some measurement error for ^{15}N enriched field samples, but also from natural variability in space and time for processes sensitive to species composition and environmental factors.

5. Conclusions

Tidepools demonstrated a range of prokaryotic and eukaryotic nitrogen metabolisms that varied with animal presence and the time of day, echoing other recent studies that demonstrate marine animals serve as sites for a diversity of nitrogen metabolisms (Fiore et al. 2010, Heisterkamp et al. 2013). The ubiquity in the coastal environment of the flora and fauna found in tidepools suggests that microbial nitrogen transformations are not unique to tidepools but a general feature associated with macrobiota. The relatively high variability in the estimates of all microbial nitrogen transformations we documented is paralleled by variability in the environmental variables (e.g. oxygen, pH, temperature, species composition) that may also foster a rich mosaic of tidepool microsites for microbial biogeochemical processing and nitrogen regeneration and retention. Scaling up to the entire rocky shore ecosystem suggests a large potential role for animals in ameliorating fluctuations in upwelling and nutrient delivery. Meanwhile, ongoing animal harvest in ocean systems has greatly impacted nitrogen cycling (e.g. Maranger et al. 2008), making it imperative to understand the links between nitrogen in coastal systems and animal harvest.

Author Contribution. CAP, MA, SP designed the experiments and CAP, MA, SP carried them out and did laboratory analyses. CAP, GD, MA developed the model. CAP prepared the manuscript with contributions from all co-authors.

Acknowledgements. We thank E. Altabet, S. Betcher, B. Colson, M. Kanichy, O. Moulton, P. Zaykowski for making the field experiment a success, including R. Belanger's lab efforts. K. Krogsland provided nutrient analyses and J. Larkum laboratory isotope expertise. We thank the Makah Nation for access. Funding was provided by NSF-OCE 09-28232 (CAP), NSF-OCE 09-28152 (MAA), and a Fulbright Foreign Student Award (SP).

References

Aquilino, K. M., Bracken, M. E. S., Faubel, M. N. and Stachowicz, J. J.: Local-scale nutrient regeneration facilitates seaweed growth on wave-exposed rocky shores in an upwelling system, Limnology and Oceanography, 54(1), 309–317, doi:10.4319/lo.2009.54.1.0309, 2009.

Atkinson, C. L. and Vaughn, C. C.: Biogeochemical hotspots: temporal and spatial scaling of the impact of freshwater mussels on ecosystem function, Freshw Biol, 60(3), 563–574, doi:10.1111/fwb.12498, 2015.

Bayne, B. L. and Scullard, C.: Rates of nitrogen excretion by species of *Mytilus* (Bivalvia: Mollusca), Journal of the Marine Biological Association of the United Kingdom, 57(02), 355–369, doi:10.1017/S0025315400021809, 1977.

Beman, J. Michael, Chow, Cheryl-Emiliane, King, Andrew, Feng, Yuanyuan, Fuhrman, Jed A., Andersson, Andreas and Bates, Nicholas R.: Global declines in ocean nitrification rates as a consequence of ocean acidification, Proceedings of the National Academy of Sciences, 108, 208–213, 2011.

542 Casciotti, K. L.: Inverse kinetic isotope fractionation during bacterial nitrite oxidation,
543 Geochimica et Cosmochimica Acta, 73(7), 2061–2076, doi:10.1016/j.gca.2008.12.022,
544 2009.
545 Dortch, Q.: The interaction between ammonium and nitrate uptake in phytoplankton, 61, 183–
546 201, 1990.
547 Dugdale, R. and Goering, J.: Uptake of new and regenerated forms of nitrogen in primary
548 productivity, Limnology and Oceanography, 12(2), 196–206, 1967.
549 Fowler, D., Coyle, M., Skiba, U., Sutton, M. A., Cape, J. N., Reis, S., Sheppard, L. J., Jenkins,
550 A., Grizzetti, B., Galloway, J. N., Vitousek, P., Leach, A., Bouwman, A. F., Butterbach-
551 Bahl, K., Dentener, F., Stevenson, D., Amann, M. and Voss, M.: The global nitrogen
552 cycle in the twenty-first century, Philosophical Transactions of the Royal Society of
553 London B: Biological Sciences, 368(1621), 20130164, doi:10.1098/rstb.2013.0164, 2013.
554 Glibert, P. M., Lipschultz, F., McCarthy, James J. and Altabet, M. A.: Isotope dilution models of
555 uptake and remineralization of ammonium by marine plankton, Limnology and
556 Oceanography, 27, 639–650, 1982.
557 Granger, J., Sigman, D. M., Lehmann, M. F. and Tortell, P. D.: Nitrogen and oxygen isotope
558 fractionation during dissimilatory nitrate reduction by denitrifying bacteria, Limnol.
559 Oceanogr., 53(6), 2533–2545, doi:10.4319/lo.2008.53.6.2533, 2008.
560 Granger, J., Sigman, D. M., Rohde, M. M., Maldonado, M. T. and Tortell, P. D.: N and O
561 isotope effects during nitrate assimilation by unicellular prokaryotic and eukaryotic
562 plankton cultures, Geochimica et Cosmochimica Acta, 74(3), 1030–1040,
563 doi:10.1016/j.gca.2009.10.044, 2010.

564 Guerrero, M. A. and Jones, R. D.: Photoinhibition of marine nitrifying bacteria: wavelength-
565 dependent response, Mar Ecol Prog Ser, 141, 183–192, 1995.
566 Horrigan, S. G. and Springer, A. L.: Oceanic and estuarine ammonium oxidation: Effects of
567 light, Limnology and Oceanography, 35(2), 479–482, doi:10.4319/lo.1990.35.2.0479,
568 1990.
569 Kremer, B. P.: Metabolic implications of non-photosynthetic carbon fixation in brown
570 macroalgae, Phycologia, 20(3), 242–250, doi:10.2216/i0031-8884-20-3-242.1, 1981.
571 Lipschultz, F.: Isotope tracer methods for studies of the marine nitrogen cycle, in Nitrogen in the
572 Marine Environment (2nd Edition), edited by D. G. Capone, D. A. Bronk, M. R.
573 Mulholland, and E. J. Carpenter, pp. 1345–1384, Academic Press, San Diego. [online]
574 Available from:
575 http://www.sciencedirect.com/science/article/pii/B9780123725226000311, 2008.
576 Magalhães, C. M., Bordalo, A. A. and Wiebe, W. J.: Intertidal biofilms on rocky substratum can
577 play a major role in estuarine carbon and nutrient dynamics, Mar Ecol Prog Ser, 258,
578 275–281, doi:10.3354/meps258275, 2003.
579 Maranger, R., Caraco, N., Duhamel, J. and Amyot, M.: Nitrogen transfer from sea to land via
580 commercial fisheries, Nature Geosci, 1(2), 111–112, doi:10.1038/ngeo108, 2008.
581 Pather, S., Pfister, C. A., Post, D. M. and Altabet, M. A.: Ammonium cycling in the rocky
582 intertidal: Remineralization, removal, and retention, Limnology and Oceanography,
583 59(2), 361–372, doi:10.4319/lo.2014.59.2.0361, 2014.
584 Peterson, B. J., Bahr, M. and Kling, G. W.: A tracer investigation of nitrogen cycling in a pristine
585 tundra river, Canadian Journal of Fisheries and Aquatic Sciences, 54(10), 2361–2367,
586 1997.

587 Pfister, C. A.: Estimating competition coefficients from census data: a test with field
588 manipulations of tidepool fishes, The American Naturalist, 146(2), 271–291, 1995.
589 Pfister, C. A.: Intertidal invertebrates locally enhance primary production, Ecology, 88(7), 1647–
590 1653, doi:10.1890/06-1913.1, 2007.
591 Pfister, C. A., Altabet, M. A. and Post, D.: Animal regeneration and microbial retention of
592 nitrogen along coastal rocky shores, Ecology, 95(10), 2803–2814, doi:10.1890/13-
593 1825.1, 2014.
594 Plaganyi, E. E. and Branch, G. M.: Does the limpet *Patella cochlear* fertilize its own algal
595 garden?, Marine Ecology Progress series, 194, 113–122, 2000.
596 Risgaard-Petersen, N., Nicolaisen, M. H., Revsbech, N. P. and Lomstein, B. A.: Competition
597 between ammonia-oxidizing bacteria and benthic microalgae, Appl. Environ. Microbiol.,
598 70(9), 5528–5537, doi:10.1128/AEM.70.9.5528-5537.2004, 2004.
599 Schindler, D. E., Knapp, R. A. and Leavitt, P. R.: Alteration of nutrient cycles and algal
600 production resulting from fish introductions into mountain lakes, Ecosystems, 4(4), 308–
601 321, doi:10.1007/s10021-001-0013-4, 2001.
602 Soetaert, K., Petzoldt, T. and Dresden, T. U.: Inverse modelling, sensitivity and Monte Carlo
603 Analysis in R using package FME, Journal of Statistical Software, 33(3), 2010.
604 Soetaert, K., Cash, J. and Mazzia, F.: Solving Differential Equations in R, Springer Berlin
605 Heidelberg, Berlin, Heidelberg. [online] Available from:
606 http://link.springer.com/10.1007/978-3-642-28070-2 (Accessed 14 May 2015), 2012.
607 Subalusky, A. L., Dutton, C. L., Rosi-Marshall, E. J. and Post, D. M.: The hippopotamus
608 conveyor belt: vectors of carbon and nutrients from terrestrial grasslands to aquatic

systems in sub-Saharan Africa, Freshw Biol, 60(3), 512–525, doi:10.1111/fwb.12474, 2015.

Suchanek, T. H.: The *Mytilus californianus* community: studies on the composition, structure, organization and dynamics of a mussel bed., University of Washington, Seattle, PhD Thesis., 1979.

Tank, J. L., Rosi-Marshall, E. J., Baker, M. A. and Hall, R. O., Jr: Are rivers just big streams? A pulse method to quantify nitrogen demand in a large river, Ecology, 89(10), 2935–2945, 2008.

Taylor, R. B. and Rees, T. A. V.: Excretory products of mobile epifauna as a nitrogen source for seaweeds, Limnology and Oceanography, 43(4), 600–606, doi:10.4319/lo.1998.43.4.0600, 1998.

Thomas, T. E. and Harrison, P. J.: Effect of nitrogen supply on nitrogen uptake, accumulation and assimilation in *Porphyra perforata* (Rhodophyta), Marine Biology, 85(3), 269–278, doi:10.1007/BF00393247, 1985.

Vanni, M. J.: Nutrient cycling by animals in freshwater ecosystems, Annual Review of Ecology and Systematics, 33(1), 341–370, doi:10.1146/annurev.ecolsys.33.010802.150519, 2002.

Ward, B. B.: Nitrification, in Nitrogen in the Marine Environment, edited by D. G. Capone, D. A. Bronk, M. R. Mulholland, and E. J. Carpenter, pp. 199–262, Elsevier, Amsterdam., 2008.

Yool, A., Martin, A. P., Fernández, C. and Clark, D. R.: The significance of nitrification for oceanic new production, Nature, 447(7147), 999–1002, doi:10.1038/nature05885, 2007.

Biogeosciences Discuss., doi:10.5194/bg-2016-81, 2016
Manuscript under review for journal Biogeosciences
Published: 15 March 2016

630 Zehr, J. P. and Kudela, R. M.: Nitrogen cycle of the open ocean: from genes to ecosystems,
631 Annual Review of Marine Science, 3(1), 197–225, doi:10.1146/annurev-marine-120709-
632 142819, 2011.

633
634
635
636
637
638
639
640
641
642
643
644
645
646
647
648
649
650
651
652

Biogeosciences Discuss., doi:10.5194/bg-2016-81, 2016
Manuscript under review for journal Biogeosciences
Published: 15 March 2016

653
654 **Figure Captions**

655 Fig.1. A schematic of the nitrogen cycling model used in this study, where microbial processes
656 include *h* as ammonium oxidation, *y* as nitrate reduction, *r* and *x* are nitrite reduction and
657 oxidation, and *u* is uptake by phototrophs. These parameters are all first order rate coefficients
658 and instantaneous fluxes are the product of the parameter and its substrate concentration.
659 Remineralization, *m*, is a fixed rate. All parameters are defined in Table 1.

660

661 Fig. 2. The ending measured concentrations (in μM) for ammonium, nitrite, and nitrate and the
662 ending seawater temperature (^{o}C), percent oxygen, and pH in all experimental tidepools used for
663 the Linear Mixed Effect model results in Table 2. The right 3 panels are rates (nmol L^{-1} h^{-1})
664 estimated from the ODE model (Eqs. 2-7), including the estimated rate of remineralization (*m*)
665 and ammonium and nitrate uptake rates in experimental tidepools. The dark horizontal line is the
666 median, the box encompasses 50% of the data and the unfilled circles are outliers. The positive
667 effect of mussels (shaded bars) on these 3 rates was greatest during the day. Linear mixed effects
668 model results are in Table 4.

669

670 Fig. 3. ODE modeled ^{15}N fits to the data for 6 representative tidepools in all four enrichment
671 experiments. The ODE model was fit individually to each tidepool, designated with unique
672 colors and symbols. Measurements are shown with symbols, while model fits at each time point
673 are designated with lines; filled symbols with solid lines are 3 separate tidepools with mussels,
674 while open symbols with dashed lines are 3 tidepools where mussels were removed. The lines
675 thus represent the differential equation model (Eqs. 2-7) fit based on the modCost function using
676 sum of squares. The symbols are the measured values (in nmol ^{15}N L^{-1}) for the corresponding

Biogeosciences Discuss., doi:10.5194/bg-2016-81, 2016
Manuscript under review for journal Biogeosciences
Published: 15 March 2016

677 tidepool at each time point; note difference in axes for nitrite. Note that although tidepools
678 differed greatly in their nutrient dynamics, the model fits are generally close to the measured
679 value.
680
681 Fig. 4. The relationship between the predicted total ^{15}N (in nmol L^{-1}) (by the ODE model) and
682 observed quantity of total ^{15}N (in nmol L^{-1}) at the end of each of the $^{15}NH_4$ and $^{15}NO_3$ tracer
683 experiments. The 1:1 line is shown and indicates that the model did not, on average, lead to an
684 artificial production or loss of ^{15}N and thus provided a reasonable fit to overall ^{15}N dynamics.
685 Each estimate is per tidepool and filled symbols are night, while unfilled symbols are day.
686
687 Fig. 5. The estimated rates (nmol L^{-1} h^{-1}) of microbial nitrogen transformations based on the
688 ODE model in the left panel (Eqs. 2-7) and the source-product model (Eq. 1; e.g. Lipschultz
689 2008) on the right. A. ammonium oxidation ($h\bar{A}$), B. nitrite oxidation ($x\overline{Ni}$), c. nitrate reduction
690 ($y\overline{Na}$), d. nitrite reduction ($r\,\overline{Ni}$). Note differences in axes; the differential equation model rates
691 are shown at 4 times the scale of the source-sink model. All other legend elements as in Fig. 2.
692
693
694
695
696
697

Biogeosciences Discuss., doi:10.5194/bg-2016-81, 2016
Manuscript under review for journal Biogeosciences
Published: 15 March 2016

698 Fig. 1

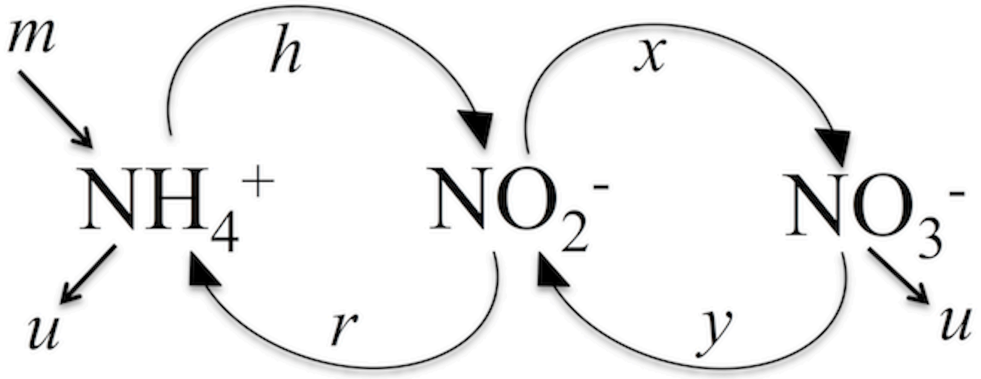

699

700

Biogeosciences Discuss., doi:10.5194/bg-2016-81, 2016
Manuscript under review for journal Biogeosciences
Published: 15 March 2016

701 Fig. 2

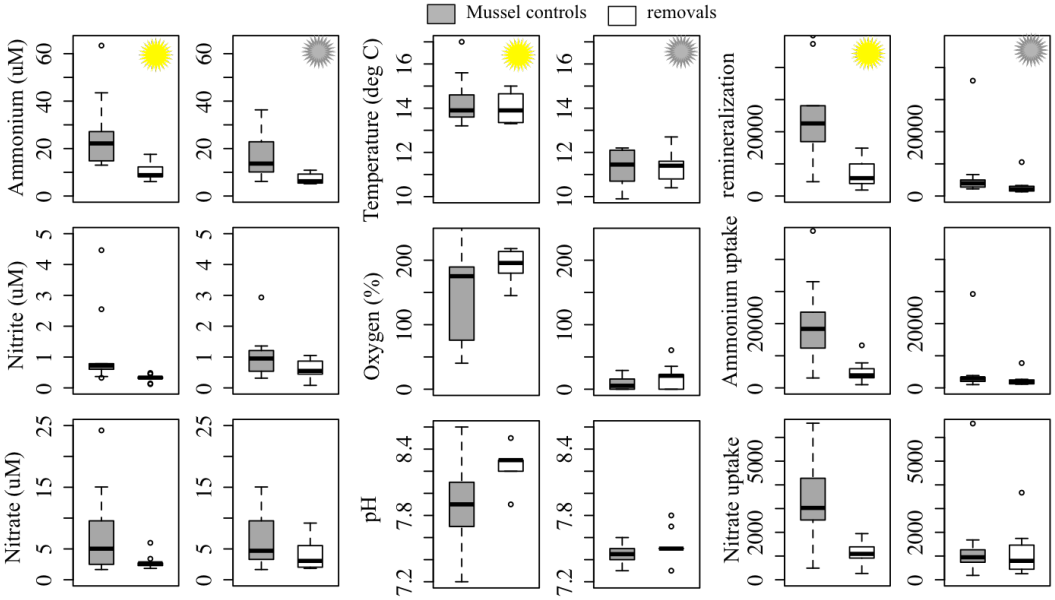

702

703

704

705

706

707

708

709

710

711

712

713

714

Biogeosciences Discuss., doi:10.5194/bg-2016-81, 2016
Manuscript under review for journal Biogeosciences
Published: 15 March 2016

715 Fig. 3

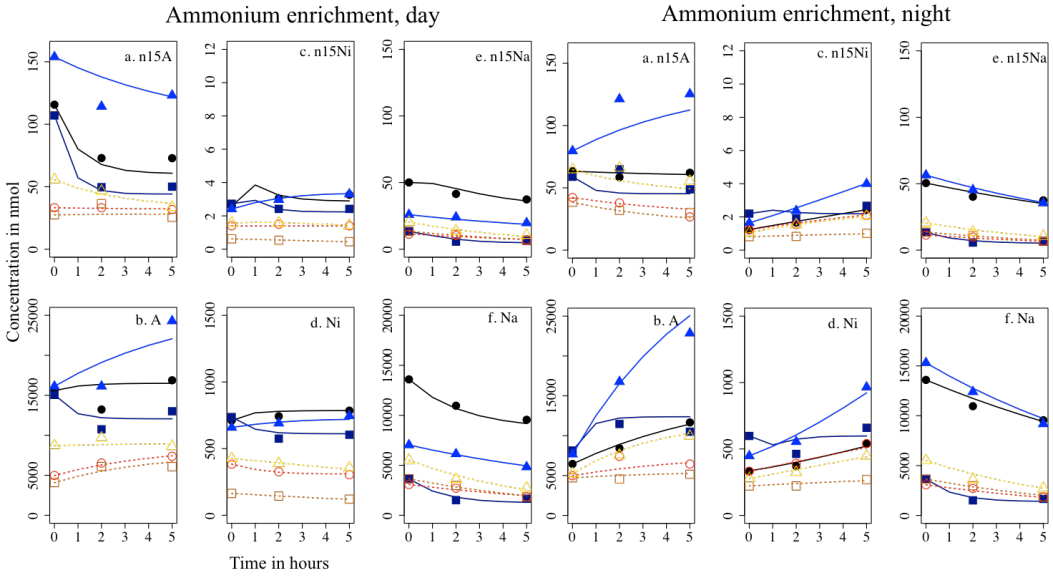

716

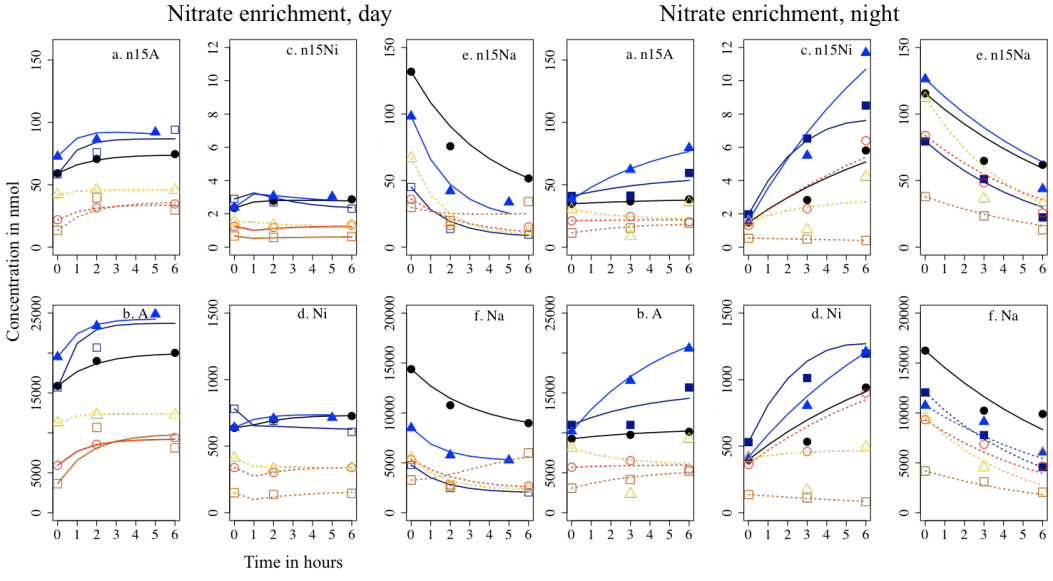

717

Biogeosciences Discuss., doi:10.5194/bg-2016-81, 2016
Manuscript under review for journal Biogeosciences
Published: 15 March 2016

Fig.4

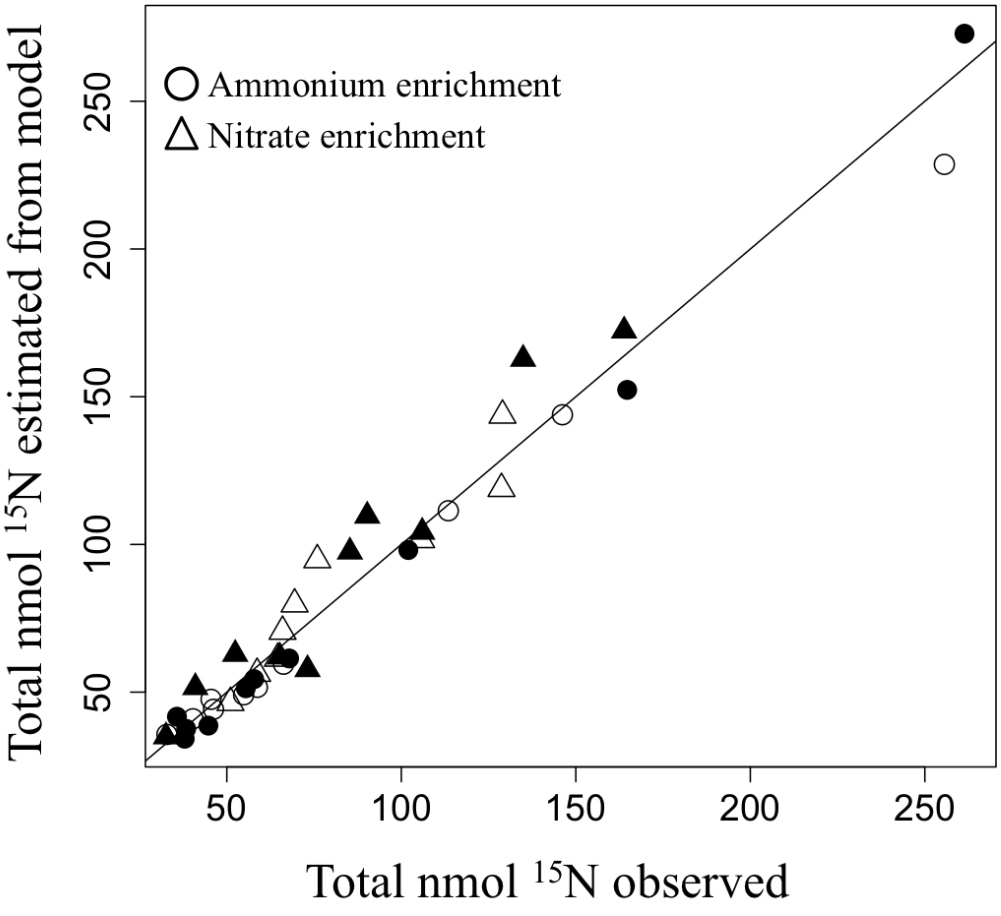

Biogeosciences Discuss., doi:10.5194/bg-2016-81, 2016
Manuscript under review for journal Biogeosciences
Published: 15 March 2016

Fig. 5

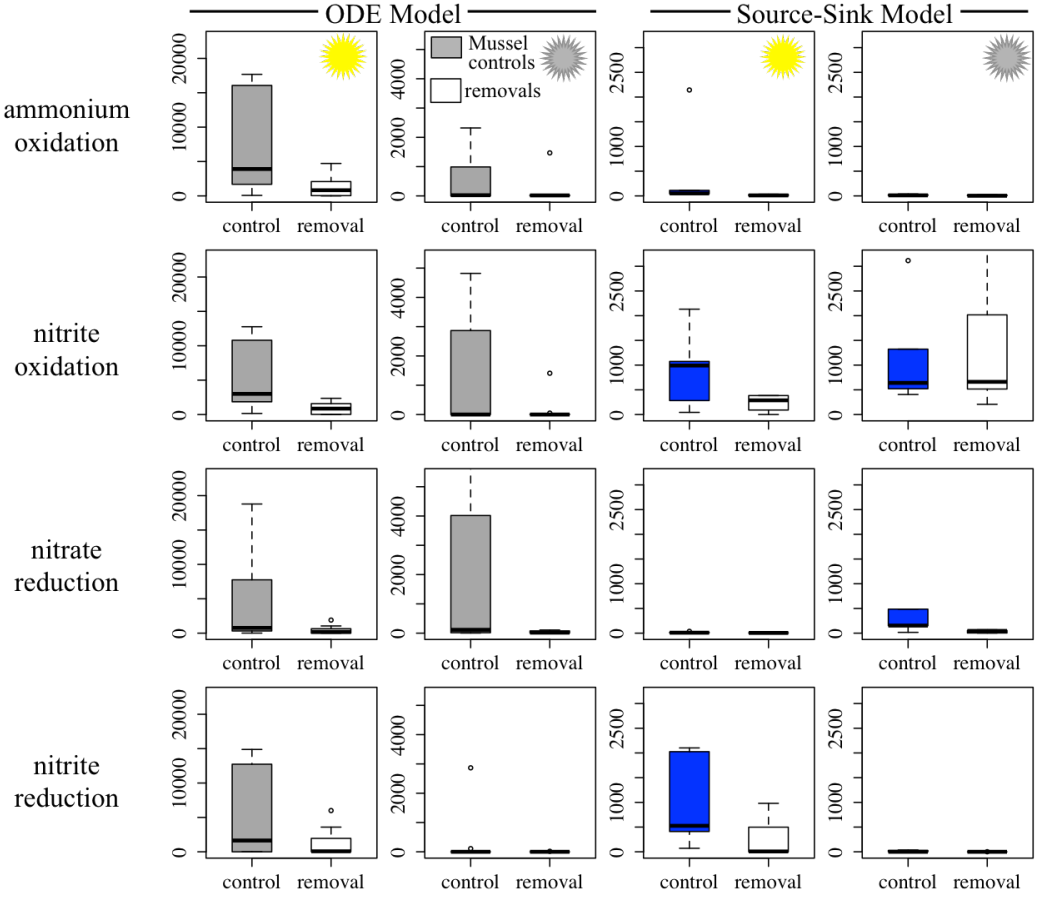

Biogeosciences Discuss., doi:10.5194/bg-2016-81, 2016
Manuscript under review for journal Biogeosciences
Published: 15 March 2016

Table 1. A list of observed and modeled parameters used in this study.

Parameter	Definition	Method of estimation
$\delta^{15}N‰$	$[(R_{sample}- R_{atmN2})/R_{atmN2}]$ x1000, where R is $^{15}N/^{14}N$	Direct experimental measurement
A	ammonium concentration (nmol L^{-1})	Direct experimental measurement
Ni	nitrite concentration (nmol L^{-1})	Direct experimental measurement
Na	nitrate concentration (nmol L^{-1})	Direct experimental measurement
n15A	nmol L^{-1} of $^{15}NH_4$	Direct experimental measurement
n15Ni	nmol L^{-1} of $^{15}NO_2$	Direct experimental measurement
n15Na	nmol L^{-1} of $^{15}NO_3$	Direct experimental measurement
R_A	Atom % ratio of $^{15}NH_4$ or n15A/A x100	Direct experimental measurement
R_{Ni}	Atom % ratio of $^{15}NO_2$ or n15Ni/Ni x100	Direct experimental measurement
R_{Na}	Atom % ratio of $^{15}NO_3$ or n15Na/Na x100	Direct experimental measurement
m	Remineralization rate (h^{-1} L^{-1})	Estimated with ODE model
u	Uptake rate coefficient (h^{-1})	Estimated with ODE model
h	Ammonium oxidation rate coefficient (h^{-1})	Estimated with ODE model
x	Nitrite oxidation rate coefficient (h^{-1})	Estimated with ODE model
r	Nitrite reduction rate coefficient (h^{-1})	Estimated with ODE model
y	Nitrate reduction rate coefficient (h^{-1})	Estimated with ODE model

Biogeosciences Discuss., doi:10.5194/bg-2016-81, 2016
Manuscript under review for journal Biogeosciences
Published: 15 March 2016

Table 2. A statistical summary of the role of mussels and day versus night on resulting seawater chemistry and temperature immediately prior to tidepool re-inundation. We used linear mixed effects models with tidepool as a random effect and log-transformed estimates for nutrient concentration; t values are given; §=0.10>p>0.05*=p<0.05, **p<0.001. The number of observations was 40.

	Mussels	**Time of Day**	**Mussels* Time of Day**
$[NH_4^+]$	3.076*	4.225**	0.841
$[NO_2^-]$	2.421*	0.232	2.327*
$[NO_3^-]$	1.865§	0.327	1.086
Percent O_2	2.727*	6.913**	2.045§
Temperature	0.784	9.254**	0.950
pH	2.223§	3.716*	1.613

Biogeosciences Discuss., doi:10.5194/bg-2016-81, 2016
Manuscript under review for journal Biogeosciences
Published: 15 March 2016

Table 3. A summary of all estimated rates by treatment in the ODE model (Eqs. 2-7). Means and (se) are shown with n=10 per treatment. The contribution of microbial transformations to overall ammonium and nitrate fluxes was quantified as the percentage that microbial activity (NH_4^+ oxidation, NO_3^- reduction, NO_2^- oxidation and reduction) contributed to all nitrogen uptake, including nitrogen uptake of phototrophs (u).

Rates (nmol L^{-1} hr^{-1})	**Mussels**		**No Mussels**	
	day	Night	day	night
Ammonium oxidation ($h\overline{A}$)	11695 (5945)	490 (262)	1435 (572)	161 (145)
Nitrite oxidation ($x\overline{Ni}$)	6980 (2433)	1904 (1173)	867 (267)	148 (140)
Nitrate reduction ($y\overline{Na}$)	4548 (2098)	2261 (1284)	435 (197)	34 (12)
Nitrite reduction ($r\,\overline{Ni}$)	9170 (5281)	298 (286)	1228 (649)	2 (2)
Remineralization (m)	25079 (4554)	7082 (3229)	6471 (1308)	3017 (868)
Ammonium uptake ($2u\overline{A}$)	20414 (4103)	5279 (2676)	4904 (1131)	2405 (618)
Nitrate uptake ($u\overline{Na}$)	3206 (530)	1465 (585)	1064 (159)	1140 (324)
% ammonium flux due to microbial activity (of total)	32 (13)	12 (10)	22 (9)	3 (2)
% nitrate flux due to microbial activity (of total)	61 (9)	30 (18)	39 (14)	8 (4)

Biogeosciences Discuss., doi:10.5194/bg-2016-81, 2016
Manuscript under review for journal Biogeosciences
Published: 15 March 2016

Table 4. A statistical summary of the role of mussels, day versus night, and their interaction on the rates of nitrogen transformations (in nmol L^{-1} hr^{-1}) estimated in both our ODE models and the traditional source-product models. Linear mixed effects models using tidepool as a random effect were used on log-transformed or square-root transformed estimates from Eq. 2-7; t values are given; §=0.10>p>0.05, *=p<0.05, **p<0.001. The correlation between coefficients estimated from each method is shown in the last column; no coefficients were significant. There were 40 observations for the ODE model and 20 for the source-sink model.

	ODE Model Estimates			**Source-Product Model**			
Rate	Mussels	Time of Day	Mussels x Time of Day	Mussels	Time of Day	Mussels x Time of Day	**Corr**
Ammonium oxidation ($h\bar{A}$)	3.131*	4.168**	2.025*	2.568*	1.970§	2.080§	0.004
Nitrite oxidation ($x\overline{Ni}$)	2.709*	5.054**	2.232*	1.278	0.364	0.935	-0.216
Nitrate reduction ($y\overline{Na}$)	2.725*	1.205	0.774	0.761	4.103*	1.657	-0.021
Nitrite reduction ($r\,\overline{Ni}$)	2.032§	2.907*	1.209	2.561*	3.365*	1.172	-0.010
Remineralization (m)	4.139*	5.676**	2.722*				
Ammonium uptake ($2u\bar{A}$)	4.183*	5.478**	2.853*				
Nitrate uptake ($u\overline{Na}$)	3.336*	3.323 *	2.307 *				

Biogeosciences Discuss., doi:10.5194/bg-2016-81, 2016
Manuscript under review for journal Biogeosciences
Published: 15 March 2016

Appendix A1. Example dynamics of stable nitrogen isotopes ($\delta^{15}N$) of tidepool ammonium, nitrite and nitrate for 4 separate ^{15}N enrichment experiments made at different times in a single control tidepool (with mussels). We measured values prior to the addition of tracer (T_o), followed by an immediate post-tracer measurement (T_1), and an approximately 2-3 hour (T_2) and a 5-6 hour (T_3) post-tracer measurement. The left 2 panels show the addition of enriched ammonium and the resultant nitrate and nitrite enrichment, while the right 2 panels show the addition of enriched nitrate and the resultant enrichment in ammonium and nitrite. In all cases, the $\delta^{15}N$ (‰) axis scale for the enriched source is double that of the product quantities.